Laser Cladding of Nickel-based Alloy Coatings on Copper Substrates

Prabu Balu[a], Edward Rea[a], Justin Deng[b]
[a]Coherent Inc., 5100 Patrick Henry Drive, Santa Clara, CA, USA 95054; [b]Coherent Commercial Co., ltd, No.25 Lane 1000, Zhangheng Road, Pudong new area, Shanghai, China 201203

ABSTRACT

The wear resistance of high-value copper components used in the metal casting, automotive, aerospace and electrical equipment industries can be improved by applying nickel (Ni)-based coatings through laser cladding. A high-power diode laser array providing continuous power levels up to 10 kilowatts with beam-shaping optics providing a rectangular focal region of various dimensions was used to deposit Ni-based alloy coatings with controlled thickness ranging from 0.3 mm to 1.6 mm in a single pass on copper (Cu) substrates. Slotted powder feeding plates with various discrete widths delivered uniform streams of powdered metal particles entrained in a carrier gas, matching the selected focal spot dimensions. To enhance laser beam coupling with the substrate and to avoid defects such as cracks, delamination and porosity, Cu substrates were preheated to a temperature of 300°C. The effect of heat input on microstructure of the cladding and extent of the heat-affected zone (HAZ) was evaluated using optical microscopy and scanning electron microscopy. Excessive heat input with longer interaction time increased dilution, porosity and expanded HAZ that significantly reduced the hardness of both the clad and the Cu substrates. Average microhardness of the Ni-C-B-Si-W alloy coating was 572 HV, which was almost 7 times greater than the hardness of the Cu substrate (84 HV).

Keywords: Laser cladding; Beam shape; Copper; Nickel; Dilution; Porosity; HAZ; Microhardness

1.0 Introduction

Copper (Cu) and its alloys are widely used in metal casting, marine, automotive and electrical equipment industries due to a combination of very high conductivity (both thermal and electrical) and good corrosion resistance. However, these materials are not good candidates for applications involving casting and rolling that demand both high wear resistance and good thermal conductivity, because of their low hardness and poor tribological properties. In order to enhance the wear resistance of Cu-based material in such applications, it is common practice to coat nickel (Ni)-based high performance materials using various techniques such as chemical plating, electro-plating, plasma transferred arc (PTA), thermal spray and laser cladding (LC). Among these techniques, both PTA and LC are capable of producing a metallurgical bond between the substrate and coating. It is reported [1] that PTA can produce thicker metal deposits with lower production costs than LC. However, the development of cost-effective, high-power direct diode laser-based cladding capable of producing deposition rates up to 30 lb/hr now makes LC competitive with PTA. Furthermore, LC with a high-power direct diode laser offers controlled heat input with increased throughput (via large-area cladding) and good wall-plug efficiency resulting in overall cost reduction when fabricating high-performance coatings.

Cu-based alloys are generally excellent reflectors and poor absorbers of visible and near-infrared light, which is typically not favorable for laser processing. The variation of the room-temperature optical absorption with wavelength for Cu and Ni is shown in Figure 1. A sharp drop in absorption for copper at a critical wavelength near 0.6 microns is evident in the graph.

It has been reported [2] that the poor absorption of readily available sources of high-power laser light by Cu-based materials can be overcome by two different approaches: 1. Pre-coating of a Cu substrate using a material with more effective optical absorption; 2. Pre-heating a Cu substrate and/or using a higher-power laser. Dehm et al. [3] performed a detailed study on laser cladding Ni-Cr-B-Si alloy on a Cu substrate using a continuous wave (CW) CO_2 laser. First, a layer of 100-µm thick Ni-Cr-B-Si alloy coating was plasma-sprayed on the Cu substrate and then the coated layer was remelted by a rectangular shaped laser beam (15 mm × 25 mm) at a scanning speed ranging from 2 to 3.3 mm/s with laser power ranging from 3.6 to 4.5 kW. Second, multiple layers (thicknesses varying from 1 mm to 2.3 mm) of Ni-Cr-B-Si alloy were coated by LC process. Their study revealed the presence of highly brittle phases (Ni_3B) in the clad leading to cracks. As a result, the coating exhibited poor wear resistance. Thicker coatings in particular tended to produce more defects such as pin holes and cracks.

In a subsequent study, Dehm et al. [4] studied laser cladding of a Co-based alloy on a Cu substrate by using a CO_2 laser. To enhance the energy coupling efficiency between mid-infrared laser irradiation and the substrate, a Cu-Ni-B-Si alloy was first plasma-sprayed on the copper. They reported that the clad exhibited both equiaxial and dendritic microstructures.

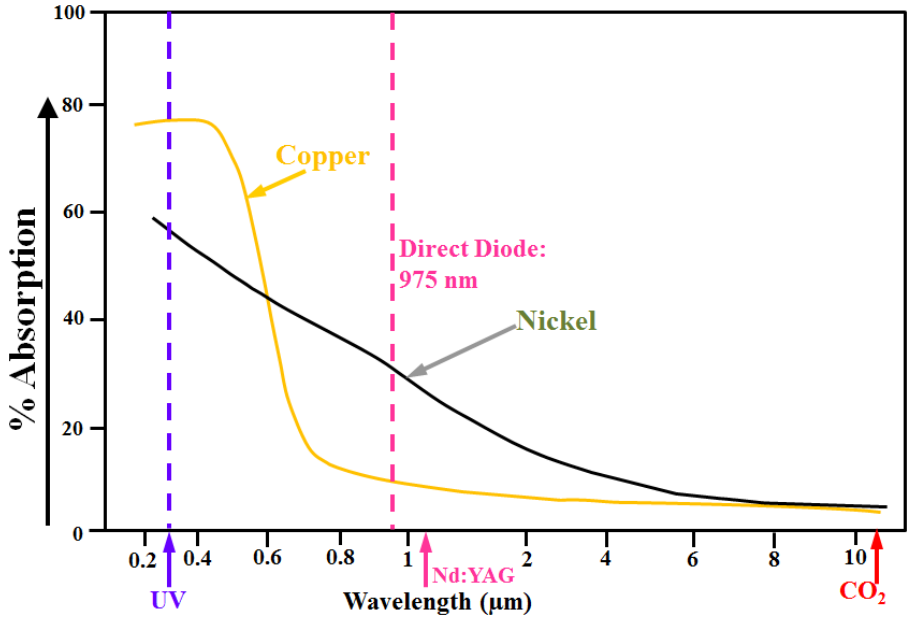

Fig. 1 – Optical absorption of copper and nickel with typical laser wavelengths indicated.

Bysakh et al. [5] performed a microstructural characterization of a laser-clad Cu-Fe-Al-Si alloy on a Cu substrate. 8 kilowatts of laser power from a 10-kW CO_2 laser at a scanning speed of 6.67 mm/s and powder mass flow rate of 8.2 g/min were used to produce the clad. It was reported that the coating microstructure was composed of Fe-rich coherent precipitates that can improve the yield strength of the coating.

Liu et al. [6] laser clad a plasma-sprayed Ni-Cu coating on a Cu substrate by using a pulsed (millisecond pulsewidth) Nd:YAG laser. A spot size of 0.3 mm with a laser power, scanning speed and overlap ratio of, 70 W, 1 mm/s and 60%, respectively were used to fabricate the samples. Hardness and wear test results revealed that the laser-clad samples exhibited 3.4X increase in hardness and 4X increase in wear resistance compared to the Cu substrate. Liu et al. [7] extended their previous study by cladding a Co-based powder (pre-placed) on top of a Ni-Cu coating. A 10-kW CO_2 laser with a spot diameter of 3 mm was used. The range of process parameters considered included: laser power=3.5-4.0 kW, scanning speed=8.3-13.3 mm/s, and overlap ratio=30%. The wear resistance of the Cu substrate -was increased 7-fold by the dual-layer coating.

Ng et al. [8] demonstrated laser cladding of a two-layer coating in which a nickel layer was sandwiched between Cu and molybdenum (Mo) substrates. A 2-kilowatt CW Nd:YAG laser with a diameter of 1 mm was used in their study. They achieved a defect-free coating for a combination of laser power=1000 W, scanning speed=15 and 12 mm/s and overlap ratio=50%.

Adak et al. [9] performed a feasibility study on the laser cladding of Cu-30Ni wire (0.8-mm diameter) on a Cu-30Ni substrate using a direct diode laser with a rectangular shaped beam of 12 mm × 0.5 mm. Laser power ranged between 3 to 4 kW, scanning speed from 2.25 to 6.85 mm/s, and wire feed rate between 29-75 mm/s. Zhang et al. [10] demonstrated the laser cladding of Ni-based alloy directly on the Cu substrate by using a CO_2 laser with a defocused spot size of 2.5 mm. The Cu substrate was preheated to a temperature of 300°C to enhance the absorption of 10.6-µm wavelength laser light. A laser power of 3.2 kW, scanning speed of 5 mm/s, and powder feed rate of 5.0 g/min was used to produce the coating. They achieved an average coating hardness of 360 HV that was about 5 times harder than the Cu substrate.

Apart from these noted citations few other studies have reported laser cladding of high performance wear-resistant coatings on a Cu substrate. In particular, the direct laser cladding of thin and thick Ni-Cr-B-Si and Ni-C-B-Si-W on a Cu substrate using a range of different focal region dimensions (6 mm x 2 mm, 6 mm x 3 mm, 6 mm x 4 mm and 12 mm x 3 mm) has not been previously reported. The main objective of this study is to obtain high-quality Ni-Cr-B-Si and Ni-C-B-Si-W coatings directly on a Cu substrate with and without preheating using a high-power

direct diode laser. In addition, the effect of different beam shapes (heat input) on the clad output quality such as dilution and porosity was studied and results are discussed in detail.

2.0 Experimental Details

Commercially available high-purity copper (C110) plates in half-hard (H02) condition with dimensions of 100 × 80 × 12.7 mm were used as substrates in this study. Ni-Cr-B-Si and the Ni-C-B-Si-W powders containing gas-atomized spherical/near-spherical metal particles as well as non-spherical (angular) carbide particles were employed. Particle sizes ranging from 53 to 180 µm were measured (see Fig. 2).

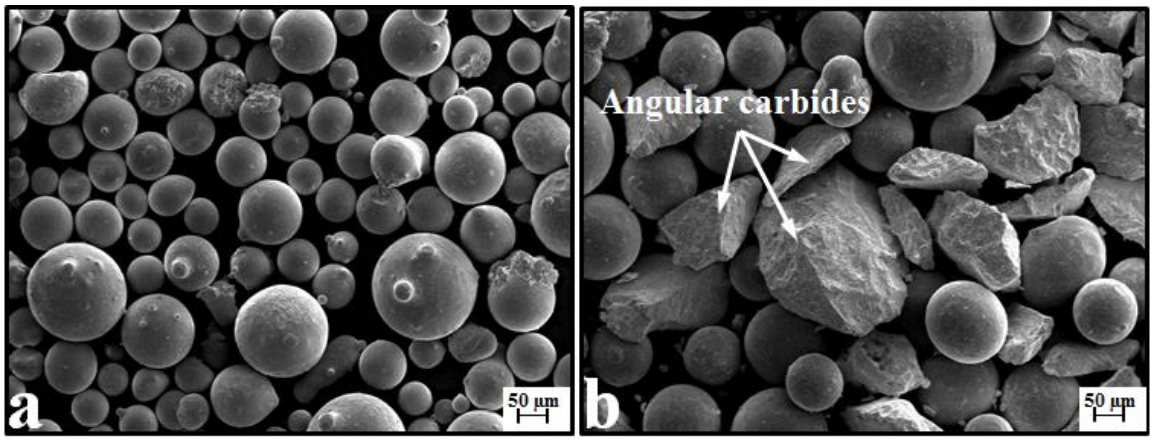

Fig. 2. - SEM images show the morphology of as received powders: (a) Ni-Cr-B-Si (b) Ni- C-B-Si-W

Chemical assays of the powders are presented in Table 1.

Table 1 Chemical composition of Ni-based alloys (wt%).

Element	B	C	Cr	Fe	Si	W	Ni
Ni-Cr-B-Si	1.6	0.25	7.5	2.5	3.5	0.0	Balance
Ni-C-B-Si-W (1559-40Ni-60WC)	1-1.25	2.5-2.55	0	0-0.4	1-1.35	57-59	Balance

A 10-kilowatt direct diode laser from Coherent Inc. (model Highlight 10000D), was used to clad Ni-based alloy coatings on Cu substrates. The cladding powder was delivered from a pressurized gas feeder through slotted powder feeding plates from opposite sides of the optical axis (centerline of the laser head) at relative angles of +/- 35 degrees. The laser head was mounted on a 6-axis robot arm, which positioned and moved the laser head relative to the stationary horizontally oriented substrates during cladding. An electrical hot plate capable of heating the substrate up to 300 $^{\circ}$C was used for preheating. Photos of the experimental equipment are shown in Fig. 3. To avoid direct back-reflections of laser light into the beam-delivery optics, the laser head was tilted 20 degrees away from normal incidence towards the scanning direction (see Fig. 3).

Table 2 Range of process parameters used in the experiments.

Process parameters	Range
Laser power (L_p)	4.5-10 kW
Scanning speed (S_s)	2.5-25 mm/s
Powder flow rate (PFR)	19-55 g/min
Pitch (P)	5-10 mm
Preheating temperature (T_p)	no preheat and 300°C
Beam shape cartridge (BSC)	6 mm×1 mm and 12 mm×1 mm
Negative lens (NL)	2, 3 and 4

Prior to laser cladding, the Cu substrate surfaces were roughened using 180-grit sandpaper then cleaned with acetone. To obtain high quality coatings (minimize porosity and cracking), the influence of LC process parameters such as laser power, scanning speed, powder flow rate and different beam sizes were investigated. Laser-

clad test samples were examined under an optical microscope and micro-hardness tester, and a reasonable range of process parameters are selected based upon the absence of excessive dilution, minimization of inter-track porosity and/or cracks, good adhesion to the deposited layer (lack of delamination) to the substrate and near-uniform microhardness.

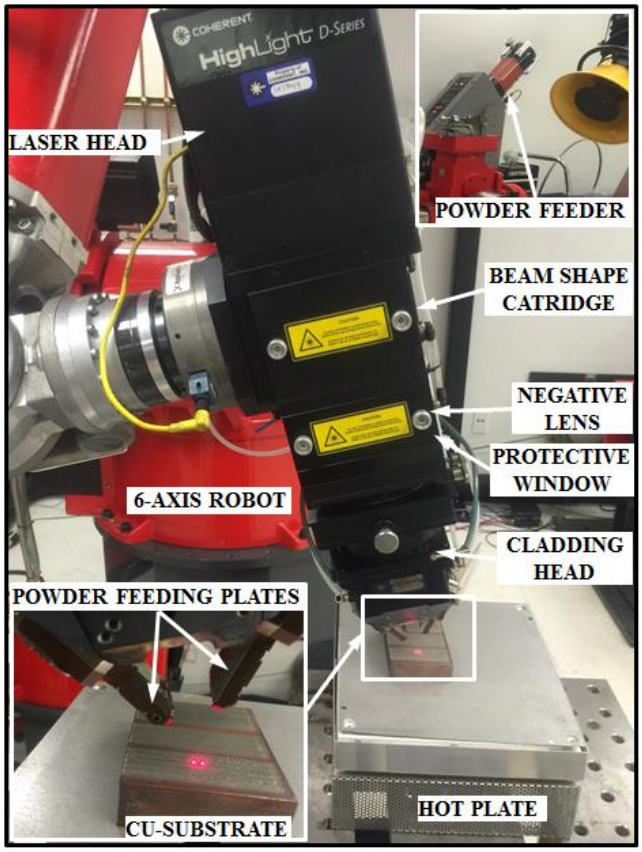

Fig. 3 - Coherent Inc. D-series 10 kilowatt direct diode laser array

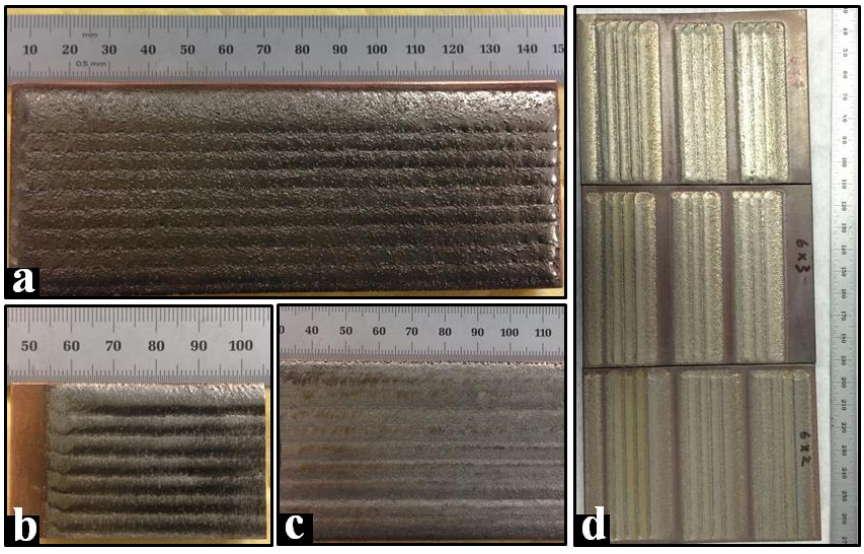

Fig, 4 - Fabricated coatings on Cu substrate: (a) thick Ni-Cr-B-Si (b) thin Ni-Cr-B-Si (c) thin Ni-C-B-Si-W (d) medium thick Ni-Cr-B-Si at different beam dimensions (6 mm×2 mm, 6 mm×3 mm, 6 mm×4 mm) and laser powers (7 kW, 8 kW and 10 kW)

The range of process parameters used in this study is presented in the Table 2. On each sample, 5 tracks of 75-mm long clads were deposited side by side at a calculated overlap ratio depending on the geometry of the clad. Figure 4 shows representative coatings of Ni-Cr-B-Si and Ni-C-B-Si-W on a Cu substrate fabricated at various process parameters.

After laser cladding, the samples were sectioned, polished and etched with a mixture of CH_3OH (100 ml), $FeCl_3$ (5g) and HCl (20 ml) solution to reveal the microstructure. Microstructure observation was performed using a measuring microscope MM-40 (Nikon, Japan). A Hitachi (S-4300) Scanning Electron Microscope (SEM) with Energy Dispersive Spectroscopy (EDS) was used to perform the microstructural and chemical compositional analyses. Micro-hardness measurements were carried out both along and across the cross-section of the coating using a MICROMET 5104 microhardness tester (Buehler, USA) with a load of 200gf at 15 sec (for Ni-Cr-B-Si) and 500gf at 15 sec (for Ni-C-B-Si-W).

3.0 Results and Discussion

Figure 5a is an SEM image showing the cross-section of a Ni-Cr-B-Si coating on a Cu substrate. A beam size of 6 mm × 2 mm, laser power of 4500 W, scanning speed of 2.5 mm/s, and powder flow rate of 21 g/min was used to fabricate the Ni-Cr-B-Si coating of thickness 1.6 mm.

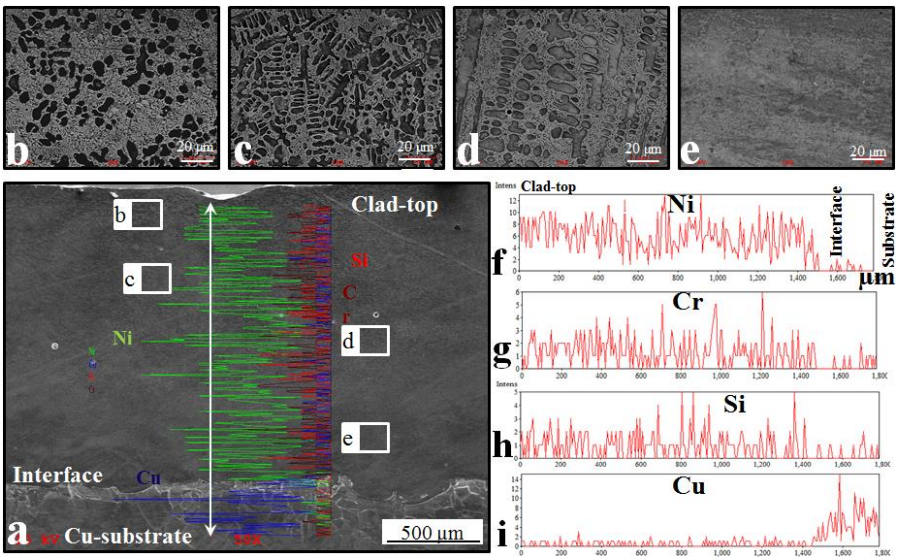

Fig. 5 - (a) SEM micrograph showing the cross-section of the Ni-Cr-B-Si coating on Cu substrate; microstructures of coating at different regions of coating: (b) near-surface (c) slightly lower (d) intermediate (e) near-substrate; EDS line-scan intensity spectrum of different alloying elements from clad top to substrate; (f) Ni (g) Cr (h) Si (i) Cu. Note that boron and carbon are not shown due to the low sensitivity of the EDS detector to light elements.

The white double-headed arrow (top to bottom) indicates the measurement line along which the elemental analysis was performed using Energy Dispersive Spectroscopy (EDS). Figures 5b through e represent the microstructure of the coating at four different regions (refer to Fig 5a). It can be seen that the coating exhibits four different microstructures at these different regions. There is a significant difference in the size of the dendrite arms and the amount of eutectic phases in the microstructure. This variation in the microstructure indicates that differences in cooling rates occur in a thick Ni-Cr-B-Si coating at different depths. For instance, a thin near-surface layer of clad solidifies rapidly by convection (shielding gas flow) as the laser beam moves away from the molten pool resulting in a fine microstructure (less time available for grain growth). A comparison of microstructures (Figs. 5b through e) reveals that the length of the dendrite arm increases towards the coating/substrate interface which indicates that the majority of heat extraction occurs towards the substrate (thickness direction). Figures 5f through i represent the variation of intensity count spectrum of Ni, Cr, Si and Cu, respectively, present in the clad as a function of distance from the top of the clad to the Cu substrate. The line-scan reveals the qualitative information about the chemical composition and distribution of elements in the clad. It can be observed from Fig. 5i that the presence of Cu in the clad remains minimal and jumps up at the interface region (~1.6 mm from the top).

Optical micrographs corresponding to the Ni-Cr-B-Si coating fabricated with no preheating at a laser power level of 10 kW, scanning speed of 10.0 mm/s, and powder flow rate of 21 g/min are presented in Figs. 6a-d. It can be observed that there are considerable differences in the grain size of the Cu substrate close to the clad=substrate interface which confirms the grain growth in the HAZ (Fig. 6a). Coating microstructure close to the fusion zone reveals a Ni-rich columnar dendritic structure with Cr-rich precipitates (Fig. 6b). The presence of Cr-rich precipitates in LC of similar material composition was also reported by Hemmati et al. [12]. The top view of the coating shows a uniform interdendritic microstructure with Cr-rich precipitates and eutectics (Figs. 6c and d). It was found that a threshold dosage of 80 J/mm^3 was required to clad Ni-Cr-B-Si coating on the Cu substrate without preheating.

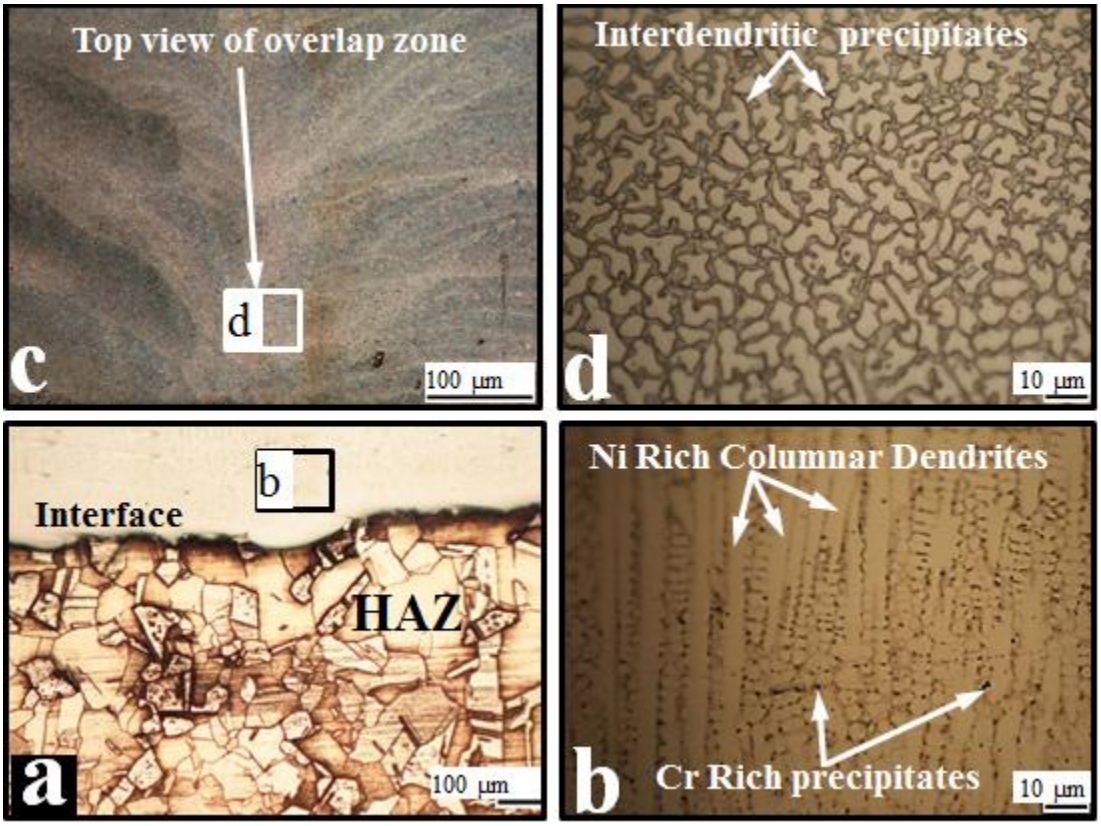

Fig. 6 - Optical micrograph showing the microstructure of the Ni-Cr-B-Si coating on Cu substrate without preheating (a) Cu substrate/coating interface region (b) coating region near interface at higher magnification (c) overlap region (d) overlap region at higher magnification

The SEM micrograph of the Ni-C-B-Si-W coating cross-section of thickness approximately 0.4 mm is shown in Fig. 7a. A laser power of 5000 W, scanning speed of 10.0 mm/s, powder flow rate of 36 g/min, and beam size of 6 mm × 2 mm was used to fabricate the coating. The coating consists of nickel matrix and uniformly distributed large tungsten carbide (WC) particles with the size up to 160 microns as shown in the Fig. 7a. Occasionally, cracks present in the coating in different directions pass through the matrix as well as the carbide particles (Fig. 7b). The surface of the carbide particles is not smooth, characterized by the traces of melting and growth from the melt carbide plates on the surface of the carbide grains. The internal structure of the carbide particle apparently characterizes the polycrystalline structure. Interestingly, the WC particles are not fragmented during the LC process that confirms that the thermal damage of WC particles is minimal (Fig. 7c). A thin layer of approximately 10 µm of fusion zone can be observed from Fig. 7d which confirms a good metallurgical bonding between the coating and substrate. Image analysis technique was used to measure the volume fraction of reinforcement (WC) and matrix (Ni-C-B-Si) in the clad and the values are 46.3% and 53.6%, respectively. The result confirms that the clad composition is consistent with the powder composition that contains 60% of WC (by mass).

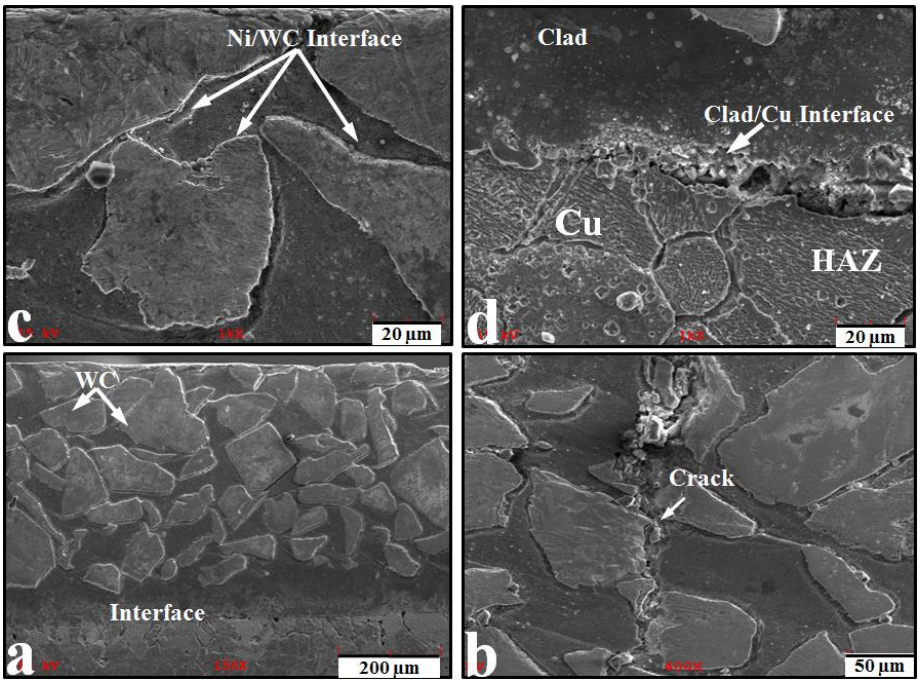

Fig. 7 - (a) SEM micrograph shows the cross-section of the Ni-C-B-Si-W coating on Cu substrate (b) higher magnification shows the crack (c) reinforcement (WC) /matrix interface, (d) substrate/Clad interface

3.1 Dilution

Dilution is a measure of clad quality that indicates the amount of mixing of substrate material in the clad material. Minimal dilution is essential to obtain metallurgical bonding between the coating and substrate. Excessive dilution leads to poor performance of the clad during service conditions. In this study, dilution is defined as follows:

$$Dilution = \frac{(x_{c+s} - x_p)}{(x_s - x_{c+s}) + (x_{c+s} - x_p)}$$

where x_{c+s}, x_p and x_s are weight percentage of Cu element in the clad + substrate, powder alloy and substrate, respectively. In each sample, the Cu content was measured by energy-dispersive spectroscopy (EDS) over an area of 0.5 mm × 0.5 mm at 3 different locations (near-surface, middle, near-substrate) and in all three 5-tracks of the coating.

The representative EDS spectrum of the thick layer of Ni-Cr-B-Si coating fabricated at a laser power of 10 kilowatts, scanning speed of 10 mm/s, powder flow rate of 55 g/min is shown in Fig. 8a. It can be seen from the spectrum that the coating composed of Ni, C, Cr, Cu, Si, and Fe. Figure 8b shows the cross section of the coating as well as the two measurement locations. It can be seen that the weight percentage of Cu element at different locations of the coating varies within 8% to 13%. Similarly, the measurements were carried out in the coatings fabricated under different process parameters and the estimated percentage of dilution varied from 6% to 65%. The maximum dilution (65%) was measured for the Ni-Cr-B-Si coating of thickness approximately 0.3 mm. The process parameters used are: laser power =10 kW, scanning speed=25 mm/s, powder flow rate=21 g/min, beam size=6 mm × 2 mm, preheating temperature=300°C. On the other hand, a lowest dilution was obtained for the following process parameters: laser power =7 kW, scanning speed=10 mm/s, powder flow rate=55 g/min, beam size=6 mm × 4 mm, preheating temperature=300°C. The cladding rate (mm^2/s) showed significant influence on the percentage of dilution rather than laser power. This can be attributed to the reduction of powder density (g/cm^2), which is the ratio of the powder flow rate to the product of the beam width and scanning speed. For instance, the dilution and powder density value corresponding to the experiments performed using the process parameters: laser power=10 kW, powder flow rate=21.0 g/min, scanning speed=25 mm/s, beam size=6 mm × 4 mm, is 52% and 0.24 $g=cm^2$, while for the same experiment with a scanning speed= 15 mm/s, the powder density is 0.39 g/cm^2 and the dilution is 30%.

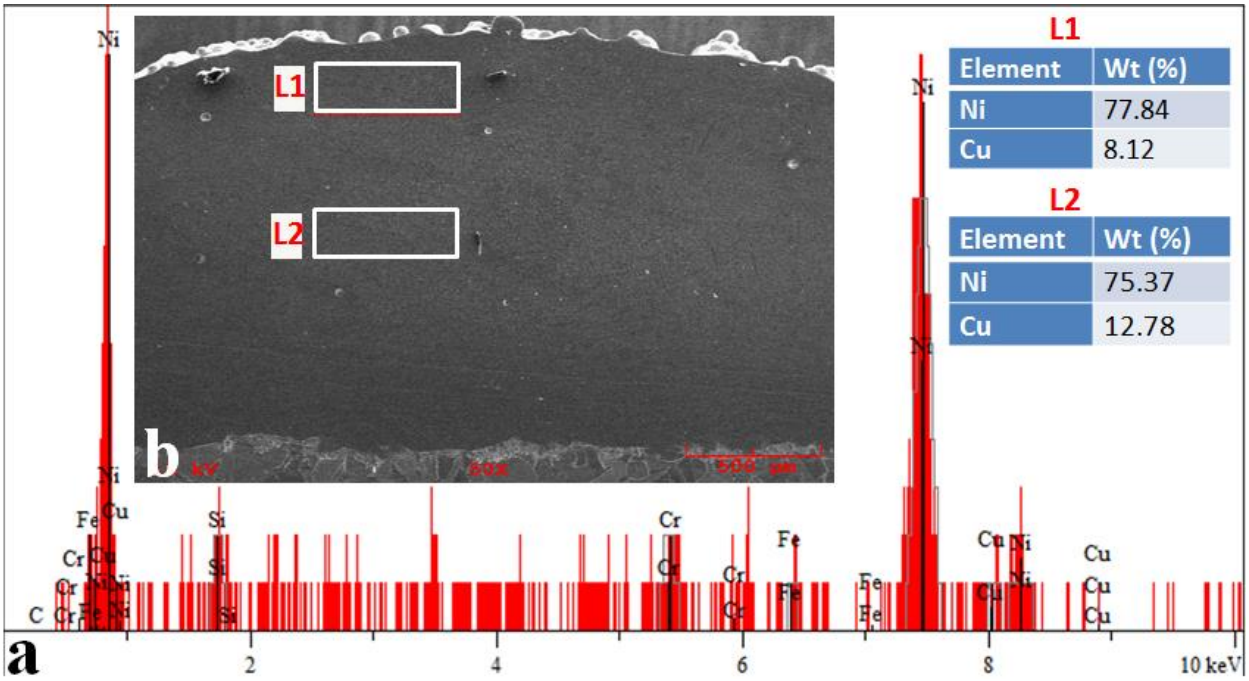

Fig. 8 - (a) Representative EDS spectrum of thick Ni-Cr-B-Si coating; (b) Cross-section indicating measurement locations.

3.2 Hardness Distribution

Hardness variations along the cross sections of thin to thick Ni-Cr-B-Si coatings and thin Ni-C-B-Si-W coatings on Cu substrates fabricated using different process parameters and different beam sizes are shown in Figs. 9a and 9b. The substrate/coating interface is marked by an axis line. The coatings presented in Fig. 9a were fabricated by a 6 mm × 4 mm beam size with a laser power of 10 kW. The thin (0.38 mm: marked by solid circle) and medium thick (0.8 mm: marked by solid triangle) coatings were produced using a scanning speed of 25 mm/s and 15 mm/s, respectively and at a powder flow rate of 21 g/min. The powder flow rate and scanning speed for thick Ni-Cr-B-Si coating (1.6 mm: marked by solid star) is 55 g/min and 5 mm/s.

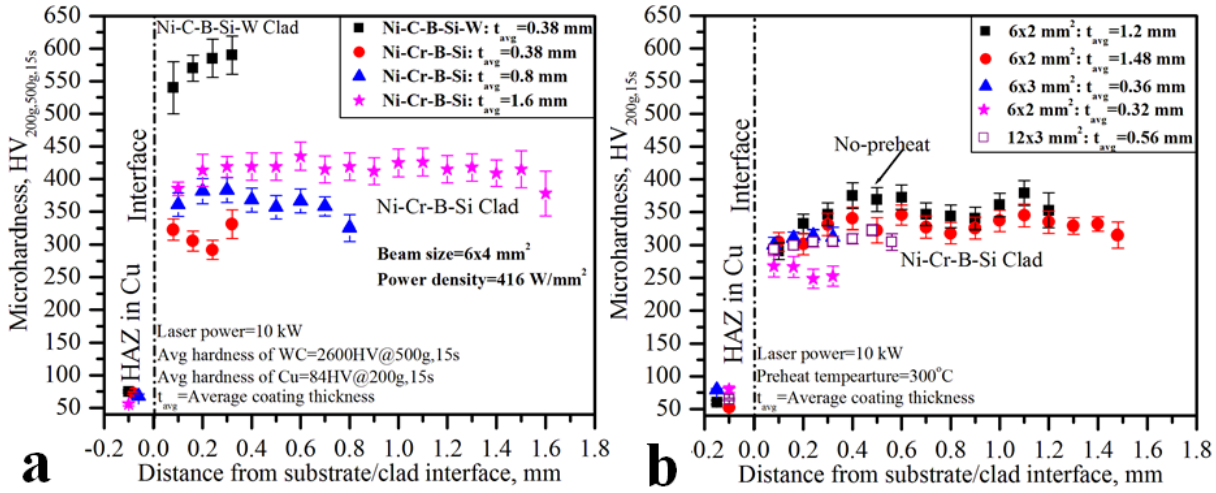

Fig. 9 - (a) Hardness variation of Ni-Cr-B-Si and Ni-C-B-Si-W coatings from bottom to top; (b) Hardness variation of Ni-Cr-B-Si coatings from bottom to top fabricated with and without preheating and different beam sizes

Three important observations can be made from Fig. 9a. First, notable hardness differences existed between various coating thicknesses and coating materials. Second, the mean hardness of matrix and reinforcement of Ni-C-B-Si-W (marked as Solid Square) is 572HV and 2600HV, respectively. Third, thick Ni-Cr-B-Si coating exhibits a

uniform hardness distribution. Further, it is worthwhile to mention that the coatings produced at slower scanning speed (5 mm/s) resulted in wider HAZ (Cu) and the mean hardness (62HV) is lower than base metal hardness (84HV). There exists an increase in the hardness values at a few measurement locations which could be attributed to the number of strengthening phases present in the Ni-Cr-B-Si alloys such as chromium borides, chromium carbides and Ni-B-Si eutectics [12]. A slight variation in the coating thickness can be noticed between the coatings fabricated with (1.48 mm: marked by solid square) and without (1.2 mm: marked by solid circle) substrate preheating i.e., the coating on the preheated substrate is thicker than the coating on the non-preheated substrate (Fig. 9b).

It can be conjectured that the preheating of Cu substrate increases the molten pool size and leads to improved powder capture efficiency. It can be noticed that the hardness of thin Ni-Cr-B-Si coating produced using a 6 mm × 2 mm size beam exhibits a minimum hardness of 225 HV which can be explained by their higher percentage of dilution (65%). A comparison of hardness variation of thin Ni-Cr-B-Si coating produced with 6 mm × 2 mm, 6 mm × 3 mm and 6 mm × 4 mm beam reveals that a combination of lower laser intensity and longer interaction time improves coating hardness. The coating produced with 12 mm × 3 mm beam showed slightly lower mean hardness that 6 mm × 3 mm beam which could be attributed to an increase in dilution with an increase in cladding rate.

3.3 Porosity measurement

The pore formation in the LC process can occur due to the presence of surface impurities, overheating of the molten pool, gas entrapment, etc. [13]. In particular, this phenomenon can occur during laser cladding of Ni-based alloys on Cu substrate since the process involves a very high solidification rate (due to the high thermal conductivity of Cu). The presence of pores in the clad can degrade the service performance of the coating.

In this study, the effect of process conditions on the formation of porosity was examined. The area porosity was measured based on digital image analysis. The fabricated coatings at different process conditions were sectioned to a dimension of 25.4 mm × 20.0 mm, ground and polished from the top surface. The total surface area of the coating was divided into equal segments of size 2.5 × 2.0 mm^2 and the percentage of area porosity was measured following the ASTM E2109-01 standard. The representative initial images captured using the optical microscope are presented in Figs. 10a and d. The initial images were first converted to grey-scale images (see Fig. 10 b & e) and then different threshold values and filters were applied to best capture the pores. Finally, image binarization (Fig. 10 c & f) was performed and the percentage area of pores was calculated.

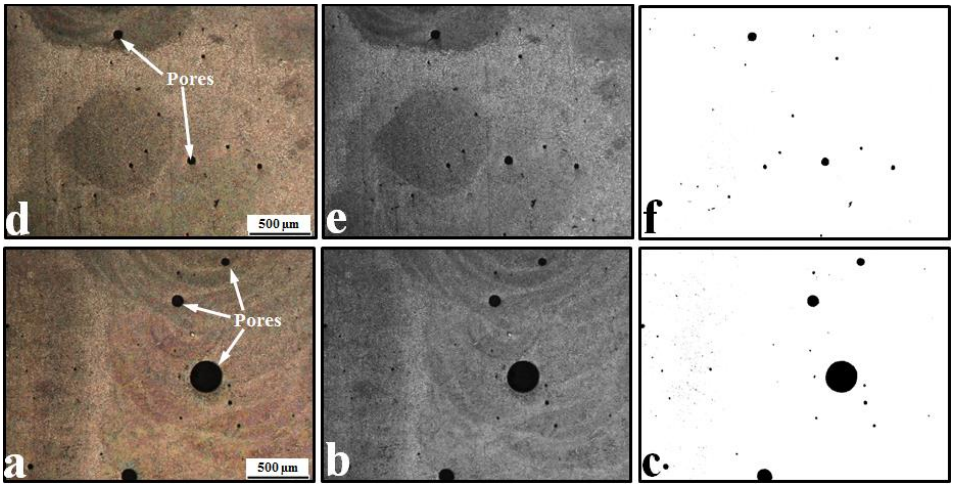

Fig. 10 - Image processing steps followed to measure the area porosity in the Ni-Cr-B-Si coatings, (a & d) Initial images of the clad, (b & e) gray scale images, (c & f) images after binarization

The procedure was followed on all samples and the measured values of area porosity were up to 4%. The thick Ni-Cr-B-Si coating produced at a laser power of 10 kW, scanning speed of 5 mm/s, powder flow rate of 55 g/min showed the maximum area porosity. The medium-thick coating fabricated with a laser power of 10 kW, scanning speed of 15 mm/s, powder flow rate of 21 g/min was free from pores and cracks. The results show that a narrow beam in the scanning direction minimizes the porosity. It can be surmised that the narrow beam results in a molten

pool with a higher aspect ratio (depth/width) which in turn minimizes the chance for the gas entrapment. In contrast, a narrow beam with higher cladding rate leads to increased dilution.

4.0 Conclusions

Laser cladding of Ni-based alloy coatings varying from 0.3 mm to 1.6 mm in thickness was successfully demonstrated on copper substrates using a high-power direct diode laser array. The following conclusions can be drawn from this study:

1. Laser cladding of Ni-based alloy coatings on copper is possible up to a cladding rate of 125 mm^2/s by using the direct diode laser of power up to 10 kW with preheating. A minimum dosage of 80J/mm^3 is required to clad Ni-based alloy on Cu substrates without preheating.
2. The measured value of percentage dilution varied over a range of 6% to 65% based on the process parameters used in the current study.
3. An average matrix hardness of Ni-C-B-Si-W coating was 572 HV which was almost 7 times larger than the Cu substrate.
4. A beam size up to 12 mm x 3 mm can be used to fabricate the Ni-based alloy coatings on the Cu substrates with a preheating temperature of 300°C.
5. The percentage of area porosity in the clad was up to 4% depending upon the process parameters. Beam size in the scanning direction significantly influences the percentage of area porosity in the coating.

5.0 Acknowledgement

The authors would like to acknowledge Mr. Paul Lee at Coherent Inc. for his help in SEM analysis and Ms. Rachel Major for the help in microhardness measurements of the samples.

6.0 References

[1] J.F. Flores, A. Neville, N. Kapur, and A. Gnanavelu , "An experimental study of the erosion–corrosion behavior of plasma transferred arc MMCs," Wear, Papers 267, 213–222 (2009).

[2] J.F. Ready, Industrial Applications of Lasers, 2nd ed., Academic Press (1997).

[3] Y. Zhang, Y. Tu, M. Xi and L. Shi, "Characterization on laser clad nickel based alloy coating on pure copper," Surface & Coating Technology, Papers 202, 5924–5928 (2008).

[4] G. Dehm, D. Medres, L. Shepeleva, C. Scheu, M. Bamberger, B.L. Mordike, S. Mordike, G. Ryk, G. Halperin, and I. Etsion, "Microstructure and tribological properties of Ni-based claddings on Cu substrates, Wear, Papers 225-229, 18–26 (1999).

[5] G. Dehm, and M. Bamberger, "Laser cladding of Co-based hardfacing on Cu substrate," Journal of Materials Science, Papers 37, 5345–5353 (2002).

[6] S. Bysakh, K. Chattopadhyay, T. Maiwald, R. Galun, and B.L. Mordike, "Microstructure evolution in laser alloyed layer of Cu-Fe-Al-Si on Cu Substrate," Materials Science and Engineering A, Papers 375-377, 661–665 (2004).

[7] F. Liu, C. Liu, S. Chen, X. Tao, Z. Xu, and M. Wang, "Pulsed Nd:YAG laser post-treatment Ni-based crack-free coating on copper substrate and its wear properties," Surface & Coating Technology, Papers 201, 6332–6339 (2007).

[8] F. Liu, C. Liu, S. Chen, X, Tao, and Y. Zhang, "Laser cladding Ni-Co duplex coating on copper substrate," Optics and Lasers in Engineering, Papers 48, 792–799 (2010).

[9] K.W. Ng, H.C. Man, F.T. Cheng, and T.M. Yue, "Laser cladding of copper with molybdenum for wear resistance enhancement in electrical contacts," Wear, Papers 253, 6236–6241(2007).

[10] B. Adak, P. Nash, and D. Chen, "Microstructural characterization of laser cladding of Cu-30Ni," Journal of Materials Science, Papers 40, 2051–2054 (2005).

[11] H. Yan, A. Wang, K. Xu, W. Wang, and Z. Huang, "Microstructure and interfacial evaluation of Co-based alloy coating on copper by pulsed Nd:YAG multilayer cladding," Journal of Alloys and Compounds, Papers 505, 645–653 (2010).

[12] I. Hemmati, V. Ocelik, and J. Th. M. De. Hosson, "Effects of alloy composition on phase constitution and properties of laser deposited Ni-Cr-B-Si coatings," Physics Procedia, Papers 41, 302–311 (2013).

[13] G. Buza, V. Jano, M. Sveda, O. Verezub, Z. Kalazi, G. Kaptay and A. Roosz, "On the possible mechanisms of porosity formation during laser melt injection technology," Materials Science Forum, Papers 589, 79–84 (2008).